

Temporal Profile Analysis of Sentinel-1 Image to Identify T. Aman Rice Varieties in the Coastal Region of Bangladesh

Mst. Shetara Yesmin^{1,2*}, Dipanwita Haldar³, Debjit Roy², Md. Belal Hossain²,
Priya Lal Chandra Paul², Md. Anisur Rahman⁴, Arafat Shahriar⁵

¹School of Agriculture and Environmental Science, University of Southern Queensland, Toowoomba, Australia

²Irrigation and Water Management Division, Bangladesh Rice Research Institute (BRRI), Gazipur, Bangladesh

³ASD, IIRS-ISRO, Dehradun, India

⁴Center for Natural Resource Studies (CNRS), Dhaka, Bangladesh

⁵Department of Economics, University of Chittagong, Chittagong, Bangladesh

Email: *shetara.brri.bd@gmail.com

How to cite this paper: Yesmin, M.S., Haldar, D., Roy, D., Hossain, M.B., Paul, P.L.C., Rahman, M.A. and Shahriar, A. (2025) Temporal Profile Analysis of Sentinel-1 Image to Identify T. Aman Rice Varieties in the Coastal Region of Bangladesh. *Journal of Geographic Information System*, 17, 361-380.
<https://doi.org/10.4236/jgis.2025.176017>

Received: October 21, 2025

Accepted: December 7, 2025

Published: December 10, 2025

Copyright © 2025 by author(s) and Scientific Research Publishing Inc. This work is licensed under the Creative Commons Attribution International License (CC BY 4.0).

<http://creativecommons.org/licenses/by/4.0/>



Open Access

Abstract

Monitoring of seasonal crop area, type and variety is essential for national agricultural planning and ensuring food security. Remote sensing and GIS-based satellite image analysis offer an effective and cost-efficient way to assess temporal land cover changes. This study utilized multi-temporal Sentinel-1 SAR (Synthetic Aperture Radar) time series data that have less cloud coverage and capture pigment-based properties, for proposing an effective method of mapping T. Aman rice varieties during the wet season (July-December) of 2019 in the south-west coastal region of Bangladesh. First, the temporal variation of Sentinel-1 SAR backscattering coefficients (σ^0) over agricultural plots was analyzed to identify the most effective metrics for detecting and distinguishing rice fields. Sentinel-1 SAR data from five dates of transplanting at approximately 15-day intervals were downloaded from the Alaska Satellite Facility (ASF) for the period between 12 July 2019 and 22 September 2019. Following preprocessing by Sentinel Application Platform (SNAP) software, generating a temporal profile for the rice versus rice and other features were extracted with the help of QGIS land use land cover (LULC) mapping. An attempt was made to discriminate rice fields by analyzing SAR data and by a knowledge-based decision tree classification through Environment for Visualizing Images (ENVI) software. The accuracy of the mangrove forest, homestead, river, and water-logged categories was found to be more than 90%, and the accuracy of all rice types was found to be more than 80%. The overall accuracy achieved was 76.3%. Among the analyzed varieties, BRRI dhan49 showed the highest VH-polarized

backscatter (approximately -17.5 dB) during the vegetative to maturity transition, clearly distinguishing it from the other T. Aman varieties. The distinct SAR backscatter signatures demonstrated the potential of multi-temporal Sentinel-1 data for identifying T. Aman rice varieties in the coastal region of Bangladesh.

Keywords

Sentinel-1 Synthetic Aperture Radar, Rice Classification, Multi-Temporal Analysis, Decision Tree Classification, Agricultural Monitoring

1. Introduction

Sustainable crop production is vital for achieving global food security, particularly in countries like Bangladesh, where agriculture forms the backbone of the economy [1]. Among staple crops, rice holds unmatched importance in Bangladesh economically, politically, and socially. It accounts for 70% of the daily caloric intake and 56% of protein consumption [2]. Rice cultivation occupies approximately 78% of the country's total agricultural land, producing around 36.3 million tons annually. In terms of the national economy, rice contributes 46% to the crop sector GDP and 5% to the total GDP. This makes rice production central to the country's food security and development. Among Bangladesh's three primary rice-growing seasons (Aus, Aman, and Boro), transplanted Aman (T. Aman) ranks second in both cultivated area and overall production. Grown predominantly in the monsoon season (July-December), T. Aman is largely rain-fed and is well-adapted to the flood-prone and coastal areas of southern Bangladesh [3]. Its significance is particularly high in saline-prone regions where other crops may not grow well. Farmers in these regions rely on T. Aman rice as a primary source of food and income. Accurate monitoring of T. Aman production is essential for food security planning. Traditionally, crop monitoring and mapping in Bangladesh have depended on field surveys, which are time-consuming, expensive, and difficult to carry out over large or remote areas. Moreover, such surveys are not ideal for real-time monitoring and rapid decision-making [4].

Remote sensing technologies, especially satellite-based systems, provide consistent, precise, and scalable data for agricultural monitoring. However, optical satellite sensors, such as those on Sentinel-2 or Landsat, are limited during the monsoon season due to persistent cloud cover, particularly from July to September, which is the key growing phase for T. Aman rice [5]. This limitation significantly hampers optical monitoring in monsoon-affected regions like Bangladesh. In contrast, Synthetic Aperture Radar (SAR) systems, such as those on Sentinel-1 satellites, overcome this limitation by operating in the microwave spectrum [6]. SAR sensors are capable of penetrating cloud cover and acquiring data continuously, both day and night, under all weather conditions. Sentinel-1's C-band SAR is highly sensitive to surface characteristics such as water content, soil roughness,

and vegetation structure, which makes it particularly suitable for rice monitoring in coastal and flood-prone areas [7]. Rice fields, especially lowland rain-fed types like T. Aman, exhibit unique temporal backscatter signatures across their growth cycle. As the rice plants grow, changes in plant height, density, and water content cause distinct variations in SAR backscatter values. By capturing and analyzing this multi-temporal SAR data, it becomes possible to identify rice fields, monitor their growth stages, and assess crop condition [8] [9]. This approach has proven useful in mapping rice, especially when using time series analysis to detect phenological patterns. Numerous international studies have effectively utilized SAR data for monitoring rice crops. In Indonesia, multi-temporal ERS-1 C-band SAR data were used to identify rice-growing areas [10] [11]. In France, Sentinel-1 SAR was applied for large-scale rice classification [12] [13]. In Vietnam, multi-temporal SAR imagery supported yield estimation [14]. In Bangladesh, [15] used RADARSAT-1 C-band data to map Aman rice based on water depth classification. However, most of these studies, including those integrating Sentinel-1 and Sentinel-2 data [16] [17], focused on identifying general rice areas, estimating yield, or assessing field conditions, but not on classifying rice varieties. This reveals a further study in rice monitoring, particularly in variety-specific classification using SAR data. Identifying different T. Aman varieties cultivated across Bangladesh's coastal zones is critical for policy decision-making. Different rice varieties may respond differently to salinity, waterlogging, and other stress conditions. Hence, distinguishing varieties through satellite data could support targeted management, improve yield forecasting, and guide breeding programs and extension services.

The current study addressed this gap by using multi-temporal Sentinel-1 SAR data to develop a time-series profile for T. Aman rice and distinguish its different varieties from other land features like water bodies, urban areas, and mangroves in Dacope Upazila of Khulna district, a highly vulnerable coastal zone of Bangladesh. The workflow included SAR data preprocessing using the ESA SNAP toolbox, land use/land cover classification in QGIS, and decision tree-based classification in ENVI software. Through those processes, the present study aimed to generate clear temporal backscatter profiles unique to different T. Aman varieties. These profiles were used to classify crop fields based on rice variety, offering a more detailed and application-specific outcome than general rice mapping. Such classification has not been widely attempted in Bangladesh, especially in coastal settings.

2. Methodology

Multi-temporal Sentinel-1 SAR data were utilized in this study to differentiate T. Aman rice varieties and other land cover classes in the study area throughout the 2019 wet season. The methodology included data acquisition, preprocessing, temporal profile generation, classification, and accuracy assessment, as detailed below.

2.1. Study area

The study was conducted in Dacope Upazila, located in the Khulna district of southwestern Bangladesh, between latitudes 22.57°N and longitudes 89.51°E (Figure 1). The total area of the upazila is approximately 991.58 square kilometers, with an elevation ranging from 2 to 3 meters above mean sea level [18]. This region lies adjacent to the southern boundary of the Sundarbans mangrove forest, covering an area of 11790.13 hectares, which significantly influences its ecological and agricultural landscape [19] [20]. The climate in Dacope is humid subtropical, with hot summers and cold winters [21]. Average maximum temperatures range between 27°C and 34°C, while minimum temperatures vary from 16°C to 27°C. Over 75% of the annual rainfall occurs during the monsoon season (June to September), creating favorable conditions for rainfed T. Aman rice cultivation [22].

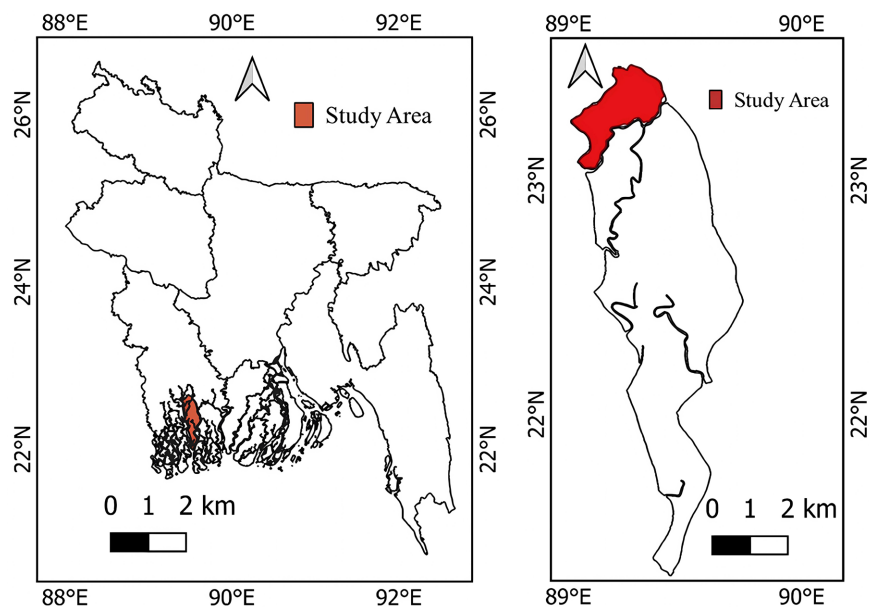


Figure 1. Location of the study area marked in orange (left) and red (right) color.

During the wet season (July-December), T. Aman rice occupied nearly 95% of this area. Farmers typically grow traditional, long-duration rice varieties with tall plant stature that are tolerant to stagnant water. These varieties are usually transplanted in August or September and harvested in December or early January. Due to their late maturity, there is a limited opportunity for a subsequent dry-season crop. During the dry season (January-May), a substantial portion of the agricultural land remains fallow, primarily due to elevated soil salinity, inadequate access to quality irrigation water, and delayed drainage conditions [23].

The region's soil is predominantly silty-clay in the top 0 - 30 cm layer, transitioning to clay at 30 - 60 cm depth [24]. Soil salinity levels fluctuate significantly between seasons, ranging from 1 - 3 dS·m⁻¹ in the wet season to 6 - 12 dS·m⁻¹ in the dry season [23]. Approximately 70% - 75% of the arable land falls within medium-high to low elevation categories, while the remaining 25% - 30% lies within

medium-high to high elevation zones [25]. This heterogeneity in elevation and salinity gradients in Dacope makes it a critical zone for studying rice cultivation under the challenging conditions of coastal regions.

2.2. Ground Truth Data Collection

Ground truth (GT) data collection took place between July and November in 2019, including GPS coordinates, varietal information for rice crops, and key phenological dates such as transplanting and harvesting. A total of six T. Aman rice varieties (BRRI dhan49, BRRI dhan75, BRRI dhan76, BR23, and local aromatic rice Sadamota) were recorded. Each variety of field growth stage was documented for temporal profile analysis. At least 60 samples were collected for each class (rice varieties, mangrove, homestead, waterbodies, and urban) to ensure statistical robustness.

2.3. Sentinel-1 SAR Data Acquisition and Preprocessing

To monitor rice growth dynamics, five Sentinel-1 SAR SLC (Single Look Complex) datasets were acquired at approximately 15-day intervals during the 2019 wet season (12 July to 22 September) from the Alaska Satellite Facility (ASF). Although the Sentinel-1 constellation typically provides a 6- or 12-day revisit frequency, images were selected at roughly 15-day intervals due to limited data availability and quality constraints over the study area. This interval ensured consistent temporal coverage that corresponded closely with key phenological stages of T. Aman rice while avoiding missing or low-quality scenes, thereby maintaining a balanced and representative time series for growth monitoring. Data preprocessing was conducted using the Sentinel Application Platform (SNAP), a widely used software suite offering specialized tools for SAR image analysis [26]. The key steps in the preprocessing pipeline are illustrated in **Figure 2**.

Preprocessing began with the conversion of SLC to Ground Range Detected (GRD) products using SNAP's "S1 SLC to GRD" operator. This step enabled the derivation of σ^0 backscatter coefficients for both VH and VV polarizations, which are crucial for analyzing vegetation and surface water dynamics [27]. Due to the coherent nature of SAR data, speckle noise is an inherent issue. To address this, multi-looking was applied, followed by a Refined Lee Filter with a 5×5 kernel [28], balancing noise reduction with edge preservation. This adaptive filtering technique is particularly effective in preserving spatial heterogeneity in rice fields, where planting density and water levels may vary [29].

Next, radiometric calibration was performed to convert digital numbers into physically meaningful backscatter values in decibels (dB), enabling comparisons across multiple acquisition dates. To reduce terrain-induced distortions, geometric corrections were applied using the Range Doppler Terrain Correction algorithm. Each scene was orthorectified using a high-resolution Digital Elevation Model (DEM) to ensure accurate ground geometry. All scenes were then precisely co-registered using SNAP's image co-registration tool, which is essential for pixel-

level alignment in time-series analyses. After radiometric and geometric corrections, VH and VV datasets were temporally stacked into a multi-date composite. To enhance signal consistency across dates and further suppress residual speckle noise, the Empirical Mode Decomposition (EMD) technique was employed [30]. This method was used to decompose complex radar backscatter time-series into intrinsic mode functions, isolating vegetation signals from short-term noise. In rice monitoring, it enhances temporal backscatter clarity by emphasizing key phenological changes such as tillering, heading, and ripening, improving the precision of variety discrimination. To minimize the effects of varying imaging conditions (e.g., changes in incidence angle, rainfall, or soil moisture), normalization of backscatter values was carried out. This process ensured consistency in the temporal profile across all acquisition dates.

These comprehensive preprocessing steps, including speckle filtering, radiometric and geometric corrections, normalization, and temporal smoothing, resulted in a clean, temporally consistent dataset. The final product was a multi-date stack of vertical transmit horizontal receive (VH) and vertical transmit vertical receive (VV) backscatter coefficients, optimized for time-series analysis. This dataset formed the basis for detecting rice phenology, tracking growth dynamics, and ultimately classifying rice varieties and other land cover types in the coastal area of Khulna.

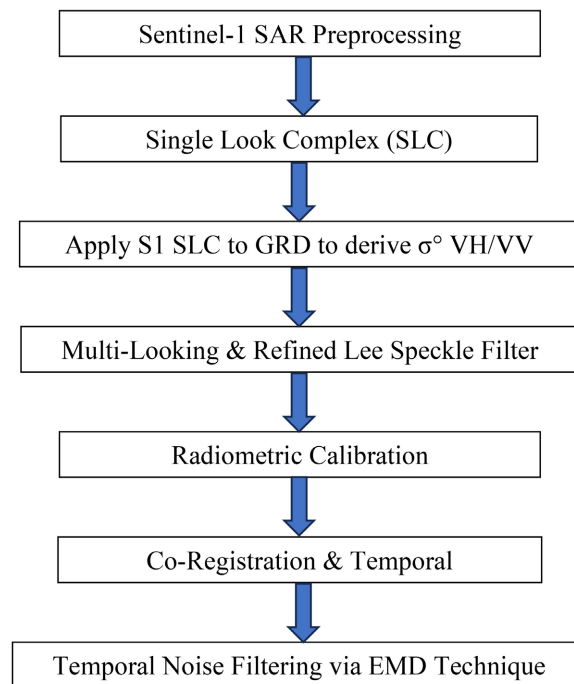


Figure 2. Flowchart of preprocessing SAR data by SNAP.

2.4. Temporal Backscatter Profile Generation

To analyze the temporal backscatter behavior of rice and other land cover types, ground truth (GT) points were collected through visual interpretation of high-res-

olution imagery and field knowledge. These GT points represented various land cover classes, including rice fields, fallow land, water bodies, homesteads, mangroves, and urban areas. The points were digitized in QGIS and exported as vector shapefiles for use in subsequent analysis. Temporal backscatter profiles were generated using Sentinel-1 SAR data, focusing on both VH and VV polarization modes. In SNAP, two sets of RGB temporal composites were developed for six acquisition dates during the 2019 wet season. The first composite covered 20 July, 5 August, and 20 August, while the second included 20 August, 5 September, and 25 September. These composites allowed visual inspection of backscatter variation across rice growth stages and supported temporal feature extraction. The vector shapefiles were imported into SNAP and overlaid on the RGB composites using the Vector Toolbox.

Subsequently, the Analysis Toolbox was used to extract statistical parameters, including mean and standard deviation of the backscatter values (in decibels), for each class and acquisition date. The extracted temporal profiles enabled the detection of distinct phenological stages in rice cultivation, such as transplanting (characterized by low VV backscatter due to water presence), vegetative growth (marked by a progressive increase in VH backscatter due to biomass accumulation), and reproductive/maturity stages (with stabilized or slightly reduced backscatter [31]). These signatures also revealed clear distinctions between rice and non-rice land covers, supporting the development of class-wise backscatter thresholds. This analysis provided a robust foundation for subsequent classification of land cover types and rice varieties using decision-tree and machine learning approaches.

2.5. Extraction and Analysis of SAR Backscatter Signatures

To support accurate land cover classification and rice variety discrimination, SAR backscatter signatures were systematically extracted and analyzed for each major land cover type present in the study area. These classes included rice fields, fallow land, water bodies, homesteads, mangrove forests, and urban settlements. Using the temporal VH and VV composites produced from Sentinel-1 data, pixel-wise backscatter values (σ°) were extracted for each class based on ground truth (GT) locations. The analysis was conducted across all six acquisition dates to capture the full seasonal variability in backscatter responses. For each land cover class, the lower and upper bounds of the σ° values were determined for every acquisition date, enabling the identification of characteristic backscatter ranges.

In the case of rice fields, phenological interpretation of these values was also performed. The lowest VV backscatter values typically occurred shortly after transplanting, when water was dominant in the field, while the highest VH values were recorded during the peak vegetative stage due to increased canopy density and volume scattering [32]. These observations allowed the construction of a temporal envelope for rice, capturing its distinct growth stages in terms of radar backscatter. For non-rice classes such as water bodies and urban areas, relatively stable backscat-

ter values across dates were observed, while mangroves and homesteads exhibited moderate temporal variability. This step of signature extraction and analysis provided essential quantitative thresholds, which were later used in the knowledge-based classification framework to differentiate between rice varieties and other land cover types based on SAR backscatter behavior over time [33].

2.6. Land Cover and Rice Variety Classification

Based on the extracted SAR backscatter thresholds for each land cover type and rice variety, a knowledge-based decision tree classifier was developed and implemented in ENVI software. This approach was selected because it allowed direct integration of expert-derived thresholds and empirical backscatter ranges obtained from field observations, making it particularly suitable for studies with limited training data and the need for transparent, interpretable classification rules. The classification rules were derived by systematically analyzing the upper and lower σ° values from both VH and VV polarizations across multiple acquisition dates [34]. These thresholds captured the temporal variability specific to rice growth stages and other land features, enabling accurate segmentation of the multi-temporal SAR composite into distinct classes. The decision tree was executed to generate a classified map representing rice varieties and various land cover types. To ensure classification reliability, the results were validated using an independent set of ground truth points. Validation metrics, including overall accuracy, kappa coefficient, and confusion matrix, were computed to evaluate performance and identify potential misclassifications [35]. Although the knowledge-based approach provided a solid foundation, integrating supervised machine learning classifiers like Random Forest and Support Vector Machines (SVM) is recommended for future improvements. These approaches would leverage labeled training datasets and apply a training-validation split to capture more complex relationships in the data.

Furthermore, a detailed analysis of VH and VV backscatter trends was conducted to observe structural and moisture-related changes in rice fields over time. The VV polarization exhibited high backscatter values during the transplanting stage due to standing water, followed by a gradual increase as canopy development progressed. In contrast, VH polarization showed increased sensitivity to biomass accumulation and canopy structure, particularly during the vegetative and reproductive stages [36]. These temporal backscatter profiles enabled the identification of key phenological transitions, such as tillering, heading, and ripening, thus facilitating rice varietal discrimination and supporting comprehensive crop growth monitoring throughout the season.

2.7. Post-Processing and Visualization

Following the classification process, post-processing and visualization were conducted to enhance interpretability and presentation of the results. Classified maps were visualized in QGIS using false-color composites, which allowed clear differ-

entiation between rice varieties and other land cover classes based on their assigned color codes. To improve spatial context and readability, cartographic enhancements were applied by overlaying administrative boundaries, hydrological networks, and other relevant thematic layers [37]. These overlays provided valuable geographic reference points, facilitating better interpretation of spatial patterns and land use distributions. The final map outputs were systematically refined to ensure clarity, consistency, and visual balance. Map elements such as legends, scale bars, and north arrows were included, and symbology was standardized across all map products. The spatial results derived from the SAR-based classification, thereby supporting informed decision-making in agricultural monitoring and sustainable land use planning.

2.8. Assessment of Accuracy by Standard Evaluation Metrics

Standard evaluation metrics (including overall accuracy, precision, recall, and F1 score) were used to measure the SAR-based rice varietal classification performance. These metrics are derived from the confusion matrix, which classifies predictions into true positives (TP), false positives (FP), false negatives (FN), and true negatives (TN). Overall accuracy measures the proportion of correctly classified samples out of the total, calculated as the sum of TP and TN divided by the total number of samples, expressed as:

$$\text{Overall Accuracy} = (\text{TP} + \text{TN}) / (\text{TP} + \text{FP} + \text{FN} + \text{TN}) \quad (1)$$

Precision, defined as $\text{TP} / (\text{TP} + \text{FP})$, measures the reliability of positive predictions by indicating the proportion of true positives among all predicted positives, thereby reflecting the rate of false positives. Recall or sensitivity, given by the formula $\text{TP} / (\text{TP} + \text{FN})$, assesses the effectiveness of the model in capturing true positive instances, thereby highlighting the rate of false negatives. As the harmonic mean of precision and recall, the F1 score is calculated by:

$$\text{F1 Score} = (2 * \text{Precision} * \text{Recall}) / (\text{Precision} + \text{Recall}) \quad (2)$$

F1 score provides a balanced metric that accounts for both false positives and false negatives in evaluating classifier performance [38]. These metrics collectively offer a comprehensive understanding of the model's classification performance, particularly in distinguishing rice varieties and land cover types using multi-temporal SAR data.

3. Results

3.1. Temporal Profile Analysis

Data from three acquisition dates were co-registered to form a unified multi-temporal dataset, reflecting spatial and temporal variations in rice planting across the study region. To generate a multi-date SAR False Color Composite (FCC) image, three acquisition dates were assigned to the primary color channels: the first date to red (R), the second to green (G), and the third to blue (B). This assignment allowed the creation of a georeferenced multi-temporal FCC dataset, visually repre-

senting temporal variations in the study area. Various types of rice varieties could easily be distinguished by the theory of color composite in RGB (Red Green Blue) format. The resulting composite images are presented in **Figure 3** and **Figure 4**.

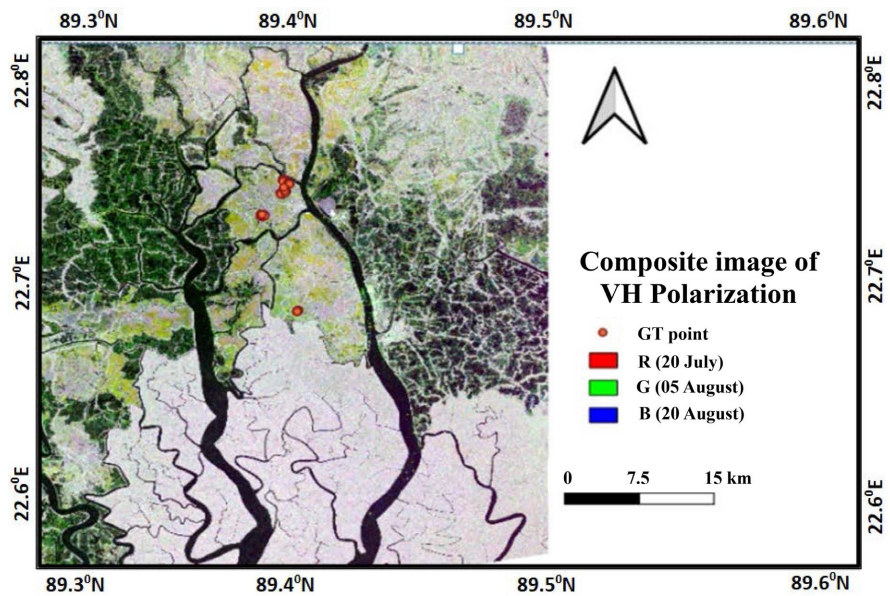


Figure 3. 1st composite (20 July, 5 August, and 20 August) of RGB image for Sentinel-1 data with ground truth (GT) points.

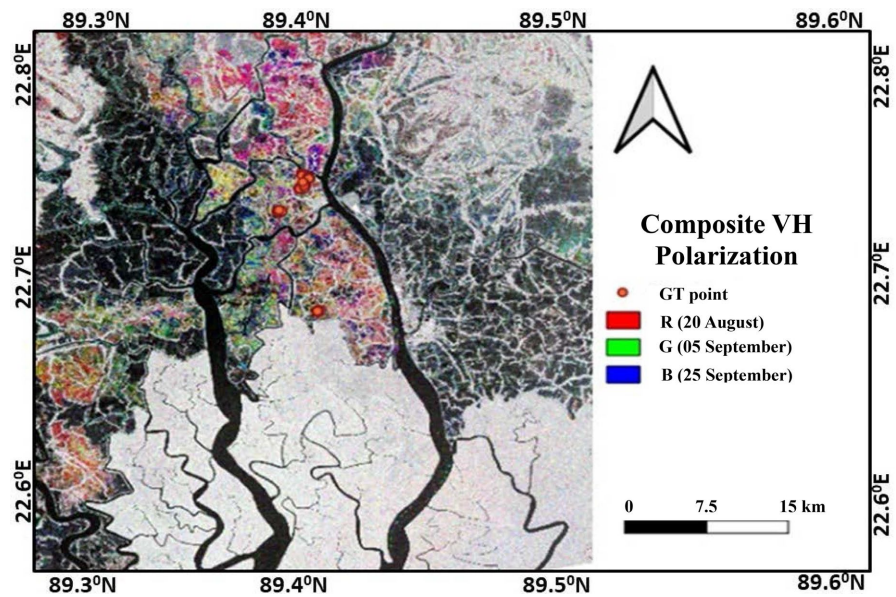


Figure 4. 2nd composite (20 August, 5 September, and 25 September) of RGB image for Sentinel-1 data with ground truth (GT) points.

3.2. Temporal Profile of All Rice vs. Other Features in VV Polarization for SAR Data

The SAR backscatter coefficient from various land-cover types was analyzed over time, as depicted in **Figure 5**. Based on analysis, the σ^0 values for all classes ex-

hibited similar variations with changes in VV polarization. The most significant increasing trend was observed in rice crop areas over time. Homestead areas in the SAR data displayed a consistently high backscatter of approximately -7 dB in VV polarization throughout the study period, appearing consistently bright across all dates with minimal variation in mean backscatter [15]. As illustrated in Figure 5, the river, characterized by its smooth surface acting as a specular reflector, exhibited very low backscatter ranging from around -21 to -23 dB [7]. Additionally, a consistent backscatter trend of -15 dB was noted for the mangrove across different dates.

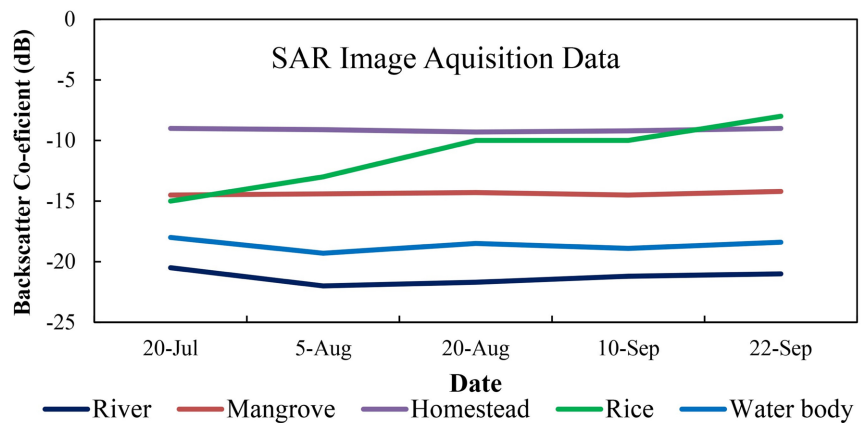


Figure 5. Temporal profile of different classes in VV polarization.

3.3. Temporal Profile of All Rice in VH Polarization

A time-series approach was applied to Sentinel-1 datasets for extracting rice areas, where the backscatter values for rice crops ranged from -25 to -15 dB (Figure 6). The backscatter values (dB) were low during the transplanting time due to flooded field conditions. Rice is usually transplanted in the field under standing water condition. At that time, rice plant height was very short, and very low backscattered values (dB) were found due to surface reflection [39]. The dB values increased

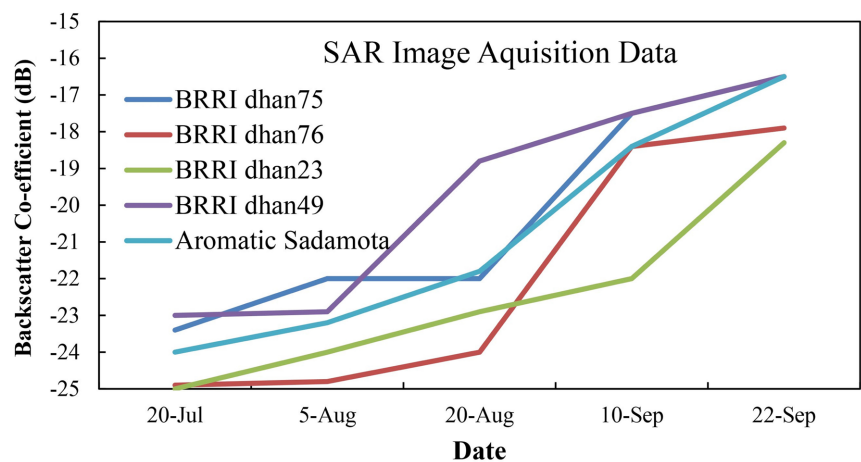


Figure 6. Temporal profile of different rice varieties in VH polarization.

progressively as the rice plants grew, reaching their peak around the mid-growth or early maturity stage [13].

3.4. Decision Tree Classification Map for SAR Data

A decision tree classification map for Synthetic Aperture Radar (SAR) data provides a visual representation of land-cover classification results obtained using a decision tree algorithm. This method segments SAR imagery into distinct categories based on decision rules derived from statistical patterns in backscatter values. The decision tree approach is widely utilized in remote sensing because of its capacity to handle non-linear relationships and accurately classify diverse land features [40].

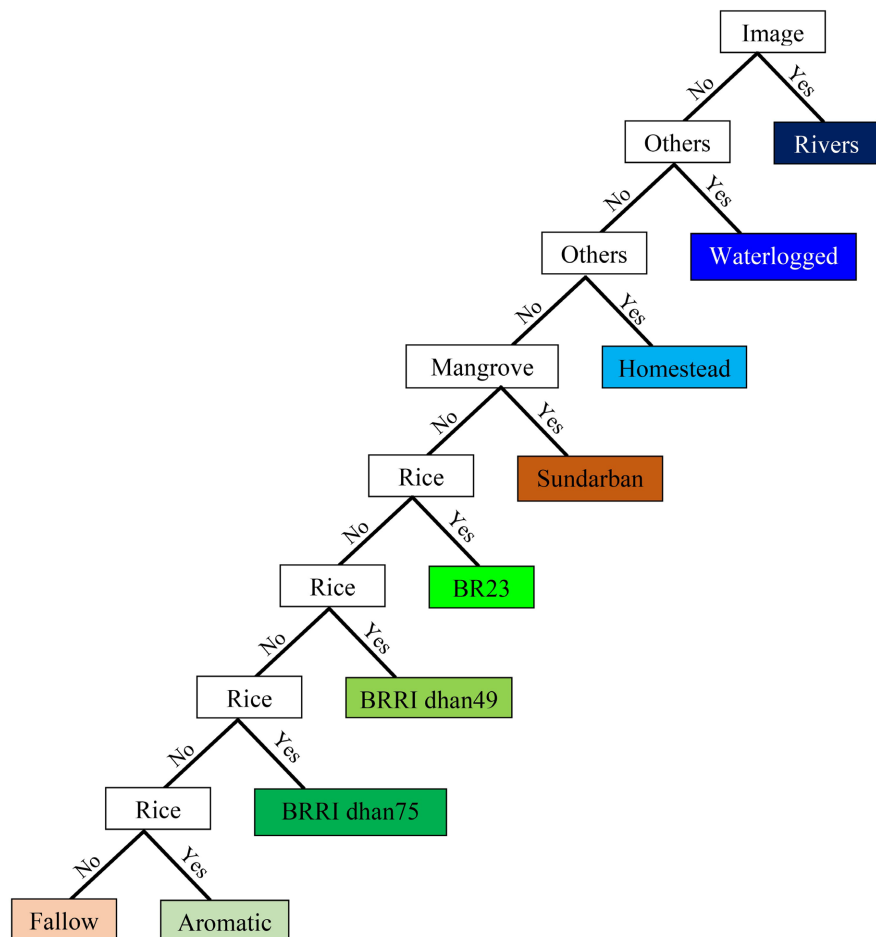


Figure 7. Decision tree classification of SAR image for different T. Aman varieties and land types.

The classification analysis successfully delineated four major land-cover types within the study area: river, waterlogged areas, homesteads, and mangroves. Moreover, distinct backscatter patterns from multi-temporal SAR data enabled the identification of various T. Aman rice varieties, including BRRI dhan75, BRRI dhan76, BRRI dhan49, BR23, and the aromatic variety Sadamota (Figure 7). The classifica-

tion utilized VH and VV polarization data from Sentinel-1, allowing precise differentiation among land covers and crop types. Multi-temporal backscatter analysis was crucial in capturing growth dynamics and surface changes over time, which improved classification accuracy [32]. The study highlights the potential of SAR-based decision tree classification for agricultural monitoring and land-use assessment. This method enhances the accuracy of rice mapping, contributing to better resource management and decision-making in rice production.

3.5. Rice Varietal Classification Map for SAR Image

Figure 8 presents the backscatter temporal profile derived from multi-temporal SAR data, enabling clear differentiation between rice categories and other land features. The mangrove class was easily identified using the VH polarization temporal profile, while other features such as homesteads, waterlogged areas, and fallow land were effectively distinguished using multi-temporal VV polarization. The classification of rice varieties was primarily based on VH backscatter polarization profiles, which helped in accurately distinguishing different rice types.

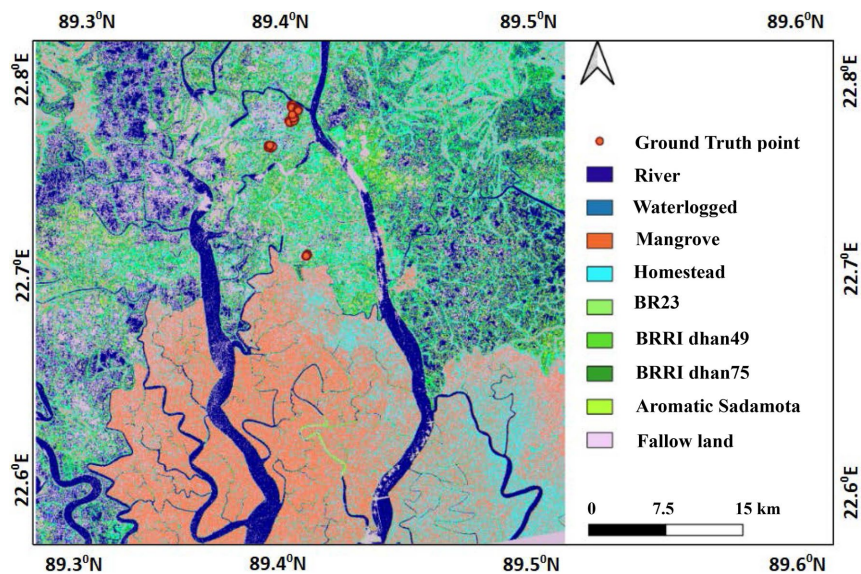


Figure 8. T. Aman rice variety classification map for SAR image.

3.6. Accuracy Assessment and Metric Analysis

Accuracy assessment was carried out using ENVI software. From the classification, the various features vs. various rice varieties showed high and significant accuracy (BRR1 dhan49 gave 81%, aromatic rice gave 83%, and BRR1 dhan75 gave 82%). The training sites, obtained from ground truth data collection, served as reference points. The results indicated that the higher level of mapping accuracy (more than 90%) was shown for the mangrove, homestead river, and waterlogged area. Whereas the accuracy of all rice types was more than 80%. The overall accuracy and kappa value were obtained 76.3% and 0.734, respectively. The accuracy of the rice varietal classification map was assessed using validation methods in-

cluding error matrices, kappa statistics, and accuracy indices. This helps assess the reliability of the classification results and identify areas of uncertainty [41].

4. Discussions

The study highlights Sentinel-1 SAR data's capability to accurately classify T. Aman rice varieties alongside other land-cover types in Bangladesh's coastal areas. The use of multi-temporal backscatter profiles enabled the differentiation of rice varieties based on their phenological stages and growth characteristics. Notably, the strong temporal variation in SAR backscatter values proved to be a reliable indicator for distinguishing rice fields from other land covers such as mangroves, homesteads, and waterlogged areas. Both rule-based and decision tree classification approaches, leveraging statistical parameters, demonstrated reliable and accurate performance, notably under conditions where optical imagery was compromised by cloud cover.

Figure 3 clearly defined that rice transplanted before 20 July gave color cyan or bluish as the first date red band gave very low backscatter (dB) value (surface reflectance) because of plant short height and flooded condition. After that, plant height increased as well as cyan color came from 2nd date green, and 3rd date blue band. Similarly, rice transplanted before 20 August gave yellowish color as 3rd date blue band. From **Figure 4**, three dates (20 August, 5 September, and 25 September) composite VH polarization gave a very clear understanding about distinguish of different types of rice by the theory of color composite in RGB format. **Figure 4** displays that before 20 August, transplanted rice gave color cyan and bluish color as red band gave very low backscatter (dB) value (surface reflectance). Before 5 September, transplanted rice gave magenta color as green band had high backscatter (dB) value (high reflection), because in that time, plants were at vegetative stage [31]. In the case of late 25 September transplanting rice, FCC color showed green in blue band with very high backscatter.

As shown in **Figure 5**, the SAR backscatter coefficient for rice increased progressively over time, forming a distinct temporal signature associated with rice crop development. The observed variation in backscatter response highlights phenological differences among rice fields in the study area [42]. This was mainly due to the crop growth of rice. **Figure 5** highlights that rice cultivation areas exhibit unique temporal SAR backscatter patterns, allowing them to be clearly distinguished from other land covers such as mangroves, homesteads, and water bodies. Likewise, non-rice areas also display distinct temporal signatures, enabling their classification [38]. Using SAR data instead of optical data offers an advantage in land cover classification because mixing in spectral signature is reduced, thereby improving accuracy [43]. This rice varietal classification map serves as a crucial tool for agricultural monitoring, crop management, and decision-making in rice-growing regions [44]. By utilizing SAR remote sensing technology, farmers, researchers, and policymakers gain enhanced capabilities to assess rice crop distribution, track growth stages, and analyze land-use patterns for better decision-

making. The use of multi-temporal SAR data enhances the precision of classification, contributing to improved crop yield estimation, resource allocation, and sustainable agricultural planning in rice-producing areas.

Analyzing the temporal profile depicted in **Figure 6**, it becomes evident that BRRI dhan49 was transplanted on 5 August, distinguished by its notably high backscattering value of -17.5 dB, facilitating its differentiation from other rice varieties [31]. The aromatic Sadamota curve demonstrates a pronounced upward trend attributable to its height and longer growth duration. In contrast, BRRI dhan75 and BRRI dhan76, transplanted before 20 July, exhibited moderate VH-polarized peaks around -18 to -19 dB, followed by a temporary decline in late August caused by heavy rainfall and waterlogging, reflecting their sensitivity to excess water and shorter phenological cycle. BR23 showed a more stable and gradually increasing VH backscatter that plateaued near -17 dB during heading, indicating uniform canopy structure and resilience under flooded conditions. These distinctive temporal signatures, ranging from the sharp peak of BRRI dhan49 to the dampened response of BRRI dhan75 or BRRI dhan76 and the steady rise of BR23 as illustrated in **Figure 6**, demonstrate the sensitivity of Sentinel-1 VH polarization to subtle structural and moisture differences among rice varieties, thus enabling accurate variety-wise discrimination [45].

However, for rice varieties like BRRI dhan75 and BRRI dhan76 transplanted before 20 July, a reduction in backscattering was observed by August 20th, attributed to field flooding from heavy rainfall. For early-sown rice, the radar backscattering coefficient shows significant temporal fluctuations across the growth cycle, suggesting dynamic phenological behavior [45]. Notably, a significant dynamic range of backscatter, varying from the initial stages of crop growth, is evident in **Figure 6**.

The study also underscores the importance of microwave remote sensing in agricultural monitoring during the wet season, where traditional optical methods fall short. The ability to identify specific rice varieties such as BRRI dhan49 and aromatic Sadamota based on their unique backscatter signatures opens new avenues for precision agriculture and crop management. By incorporating SAR data into crop classification workflows, agricultural assessments become timelier and more reliable, providing vital information necessary for safeguarding food security and optimizing resource planning.

Future Scopes

To advance the operational utility of SAR-based agricultural monitoring, several strategic recommendations emerge from this study. Initially, expanding SAR applications to other crop types and across different seasons will enable comprehensive, year-round surveillance of agricultural ecosystems. Integrating SAR with optical and multispectral datasets can enhance classification accuracy and provide deeper insights into crop health and land-use dynamics. The development of automated classification systems using machine learning models such as Random

Forests and Convolutional Neural Networks (CNNs) is essential for scaling analysis and reducing manual intervention. Policymakers should support the adoption of remote sensing technologies by investing in data infrastructure and training programs for local stakeholders. Additionally, real-time monitoring tools and forecasting dashboards based on SAR data can facilitate early detection of crop stress, flooding, and pest outbreaks, enabling timely interventions. Finally, continuous ground truth validation and engagement with farming communities are vital to ensure the relevance and accuracy of remote sensing outputs, fostering trust and practical application in agricultural decision-making.

5. Conclusions

Cropping type analysis is essential for managing resources for long-term agricultural sustainability and achieving an evergreen revolution. The primary objective of the present study was to classify the various T. Aman rice varieties and generate an enhanced land cover map. Sentinel-1 data were used for the classification. To extract reliable varietal information from the selected SAR features, a rule-based classification was performed using statistical parameters such as mean and standard deviation. Following the rule-based approach, a knowledge-based Decision Tree Classification (DTC) was constructed, and its accuracy was thoroughly evaluated. The findings highlight the substantial improvement in classifying land features, like river, homestead, mangrove, fallow land, and rice, achieved through the integration of microwave datasets. Cloud coverage and late availability of optical data were able to pick up the entire profile starting from July. Hence, SAR data was essential for carrying out this research. Using the temporal profile, BRRI dhan49 (transplanted on 5 August) could easily be separated from the other rice varieties, because of high backscattering value (-17.5 dB). The aromatic rice curve shows a high increasing trend because of the height and growth duration of the variety. However, before 20 July transplanted rice like BRRI dhan75 and BRRI dhan76, backscattering values were reduced due to flooded conditions in the field for heavy rainfall. Rice fields exhibit the strongest temporal variation in SAR backscatter relative to other land-cover classes. The research findings revealed that the SAR signature investigation enabled us to use the filtered time-series Sentinel-1 (SAR) data for identifying T. Aman rice varieties accurately during the wet season in the coastal region of Bangladesh. Varietal-level mapping can provide policymakers and agricultural agencies with actionable insights by linking spatial distribution data with management decisions. For instance, variety-specific yield forecasting enables authorities to anticipate production outcomes for high-yielding or stress-tolerant varieties such as BRRI dhan49 or BR23, allowing early planning for food supply and market stabilization. Targeted agricultural extension services can then focus on disseminating location-specific recommendations such as fertilizer management, planting schedules, or water control practices, tailored to each variety's growth duration and flood tolerance. Furthermore, accurate spatial information on varietal coverage assists in optimizing resource allocation for harvesting, stor-

age, and transportation infrastructure, ensuring that areas with high concentrations of late-maturing or high-yielding varieties receive priority logistical support during peak harvesting periods.

This capability will enable more precise decision-making for ensuring food security, improving climate resilience, and strengthening adaptive management strategies across Bangladesh's coastal agricultural systems.

Conflicts of Interest

The authors declare no conflicts of interest regarding the publication of this paper.

References

- [1] Ismail, T., Qamar, M., Khan, M., Rafique, S. and Arooj, A. (2023) Agricultural Biodiversity and Food Security: Opportunities and Challenges. In: Ismail, T., Akhtar, S. and Lazarte, C.E., Eds., *Neglected Plant Foods of South Asia: Exploring and Valorizing Nature to Feed Hunger*; Springer International Publishing, 1-27. https://doi.org/10.1007/978-3-031-37077-9_1
- [2] Jamal, M.R., Kristiansen, P., Kabir, M.J. and Lobry de Bruyn, L. (2023) Challenges and Adaptations for Resilient Rice Production under Changing Environments in Bangladesh. *Land*, **12**, Article No. 1217. <https://doi.org/10.3390/land12061217>
- [3] Islam, A.R.M.T., Nabila, I.A., Hasanuzzaman, M., Rahman, M.B., Elbeltagi, A., Mallick, J., *et al.* (2022) Variability of Climate-Induced Rice Yields in Northwest Bangladesh Using Multiple Statistical Modeling. *Theoretical and Applied Climatology*, **147**, 1263-1276. <https://doi.org/10.1007/s00704-021-03909-1>
- [4] Wu, B., Zhang, M., Zeng, H., Tian, F., Potgieter, A.B., Qin, X., *et al.* (2022) Challenges and Opportunities in Remote Sensing-Based Crop Monitoring: A Review. *National Science Review*, **10**, nwac290. <https://doi.org/10.1093/nsr/nwac290>
- [5] Shao, Y., Liao, J. and Wang, C. (2002) Analysis of Temporal Radar Backscatter of Rice: A Comparison of SAR Observations with Modeling Results. *Canadian Journal of Remote Sensing*, **28**, 128-138. <https://doi.org/10.5589/m02-019>
- [6] Chang, L., Chen, Y., Wang, J. and Chang, Y. (2020) Rice-Field Mapping with Sentinel-1a SAR Time-Series Data. *Remote Sensing*, **13**, Article No. 103. <https://doi.org/10.3390/rs13010103>
- [7] Verma, A., Kumar, A. and Lal, K. (2019) Kharif Crop Characterization Using Combination of SAR and MSI Optical Sentinel Satellite Datasets. *Journal of Earth System Science*, **128**, Article No. 230. <https://doi.org/10.1007/s12040-019-1260-0>
- [8] Choudhury, I. and Chakraborty, M. (2006) SAR Signature Investigation of Rice Crop Using RADARSAT Data. *International Journal of Remote Sensing*, **27**, 519-534. <https://doi.org/10.1080/01431160500239172>
- [9] Saha, G., Karmakar, S. and Kar, B. (2017) Quantification of N₂O Flux Density of Winter Rice as Influenced by Soil Environment. *Journal of Agrometeorology*, **19**, 1-7.
- [10] Arjasakusuma, S., Swahyu Kusuma, S., Rafif, R., Saringatin, S. and Wicaksono, P. (2020) Combination of Landsat 8 OLI and Sentinel-1 SAR Time-Series Data for Mapping Paddy Fields in Parts of West and Central Java Provinces, Indonesia. *ISPRS International Journal of Geo-Information*, **9**, Article No. 663. <https://doi.org/10.3390/ijgi9110663>
- [11] Li, M. and Bijker, W. (2019) Vegetable Classification in Indonesia Using Dynamic Time Warping of Sentinel-1a Dual Polarization SAR Time Series. *International Journal of Applied Earth Observation and Geoinformation*, **78**, 268-280.

- <https://doi.org/10.1016/j.jag.2019.01.009>
- [12] Bazzi, H., Baghdadi, N., El Hajj, M., Zribi, M., Minh, D.H.T., Ndikumana, E., *et al.* (2019) Mapping Paddy Rice Using Sentinel-1 SAR Time Series in Camargue, France. *Remote Sensing*, **11**, Article No. 887. <https://doi.org/10.3390/rs11070887>
- [13] Kurosu, T., Fujita, M. and Chiba, K. (1995) Monitoring of Rice Crop Growth from Space Using the ERS-1 C-Band SAR. *IEEE Transactions on Geoscience and Remote Sensing*, **33**, 1092-1096. <https://doi.org/10.1109/36.406698>
- [14] Phung, H.P., Nguyen, L.D., Anh Vu, N.V., Thanh, N.K. and Trung, L.V. (2022) Application of Multi-Temporal Sentinel-1 SAR Data for Yield Estimation of Rice Crops in an Giang, Vietnam. *IOP Conference Series: Earth and Environmental Science*, **964**, Article ID: 012007. <https://doi.org/10.1088/1755-1315/964/1/012007>
- [15] Panigrahy, S., Jain, V., Patnaik, C. and Parihar, J.S. (2012) Identification of Aman Rice Crop in Bangladesh Using Temporal C-Band SAR—A Feasibility Study. *Journal of the Indian Society of Remote Sensing*, **40**, 599-606. <https://doi.org/10.1007/s12524-011-0193-0>
- [16] Gao, Y., Pan, Y., Zhu, X., Li, L., Ren, S., Zhao, C., *et al.* (2023) FARM: A Fully Automated Rice Mapping Framework Combining Sentinel-1 SAR and Sentinel-2 Multi-Temporal Imagery. *Computers and Electronics in Agriculture*, **213**, Article ID: 108262. <https://doi.org/10.1016/j.compag.2023.108262>
- [17] Saadat, M., Seydi, S.T., Hasanlou, M. and Homayouni, S. (2022) A Convolutional Neural Network Method for Rice Mapping Using Time-Series of Sentinel-1 and Sentinel-2 Imagery. *Agriculture*, **12**, Article No. 2083. <https://doi.org/10.3390/agriculture12122083>
- [18] Paul, P.L.C., Bell, R.W., Barrett-Lennard, E.G. and Kabir, E. (2020) Straw Mulch and Irrigation Affect Solute Potential and Sunflower Yield in a Heavy Textured Soil in the Ganges Delta. *Agricultural Water Management*, **239**, Article ID: 106211. <https://doi.org/10.1016/j.agwat.2020.106211>
- [19] Akter, R. (2020) Indirect Effect of Climate Change on the Village Life around the Sundarbans Mangrove Forest in Bangladesh. Doctoral Dissertation, Sher-E-Bangla Agricultural University. <http://archive.saulibrary.edu.bd:8080/xmlui/handle/123456789/3760>
- [20] BBS (2019) Yearbook of Agricultural Statistics-2019. Bangladesh Bureau of Statistics.
- [21] Paul, P.L.C., Bell, R.W., Barrett-Lennard, E.G., Kabir, E. and Gaydon, D.S. (2021) Opportunities and Risks with Early Sowing of Sunflower in a Salt-Affected Coastal Region of the Ganges Delta. *Agronomy for Sustainable Development*, **41**, Article No. 39. <https://doi.org/10.1007/s13593-021-00698-9>
- [22] Islam, M.M., Ara, M.G., Roy, T. and Jahan, M.S. (2022) Adaptive Strategies of Coastal People in Response to Climate Change: Experiences from Two Villages of Dacope Upazila in Bangladesh. *Environment & Ecosystem Science*, **6**, 17-28. <https://doi.org/10.26480/ees.01.2022.17.28>
- [23] Hossain, M.B., Roy, D., Paul, P.L.C., Yesmin, M.S., Kundu, P.K., Pranto, M.R.B.H., Aklimuzzaman, M., Paul, M., Maniruzzaman, M. and Mainuddin, M. (2024) Strategies of Water Resource Utilization and Agricultural Water Management in the Coastal Saline Zone of Bangladesh. *Irrigation and Drainage*, **74**, 820-833. <https://doi.org/10.1002/ird.3022>
- [24] Paul, P.L.C., Bell, R.W., Barrett-Lennard, E.G., Roy, D., Mainuddin, M., Maniruzzaman, M., *et al.* (2024) Impact of Boro Rice Establishment Methods on Soil Salinity, Crop Growth and Yield in South-West Salt-Affected Coastal Region of Bangladesh. *Journal of the Indian Society of Coastal Agricultural Research*, **42**, 48-59.

- <https://doi.org/10.54894/jiscar.42.1.2024.146196>
- [25] Maliha, S. (2016) Changes of Land Use and Soil Properties and Their Impact on Rice Yield in Dacope Upazila of Khulna District. Master's Thesis, IWFEM, Bangladesh University of Engineering and Technology.
<http://lib.buet.ac.bd:8080/xmlui/handle/123456789/4550>
- [26] Gomasasca, M.A., Tornato, A., Spizzichino, D., Valentini, E., Taramelli, A., Satalino, G., *et al.* (2019) Sentinel for Applications in Agriculture. *The International Archives of the Photogrammetry, Remote Sensing and Spatial Information Sciences*, **3**, 91-98.
<https://doi.org/10.5194/isprs-archives-xlii-3-w6-91-2019>
- [27] Garcia, A.D.B., Islam, M.S., Prudente, V.H.R., Sanches, I.D. and Cheng, I. (2025) Irrigated Rice-Field Mapping in Brazil Using Phenological Stage Information and Optical and Microwave Remote Sensing. *Applied Computing and Geosciences*, **25**, Article ID: 100223. <https://doi.org/10.1016/j.acags.2025.100223>
- [28] Lee, J.S., Jurkevich, L., Dewaele, P., Wambacq, P. and Oosterlinck, A. (1994) Speckle Filtering of Synthetic Aperture Radar Images: A Review. *Remote Sensing Reviews*, **8**, 313-340. <https://doi.org/10.1080/02757259409532206>
- [29] Uddin, K., Matin, M.A. and Meyer, F.J. (2019) Operational Flood Mapping Using Multi-Temporal Sentinel-1 SAR Images: A Case Study from Bangladesh. *Remote Sensing*, **11**, Article No. 1581. <https://doi.org/10.3390/rs11131581>
- [30] Choudhury, I., Chakraborty, M., Santra, S.C. and Parihar, J.S. (2011) Methodology to Classify Rice Cultural Types Based on Water Regimes Using Multi-Temporal RADAR-SAT-1 Data. *International Journal of Remote Sensing*, **33**, 4135-4160.
<https://doi.org/10.1080/01431161.2011.642018>
- [31] Phan, H., Le Toan, T. and Bouvet, A. (2021) Understanding Dense Time Series of Sentinel-1 Backscatter from Rice Fields: Case Study in a Province of the Mekong Delta, Vietnam. *Remote Sensing*, **13**, Article No. 921. <https://doi.org/10.3390/rs13050921>
- [32] Fu, Y., Zhu, Z., Liu, L., Zhan, W., He, T., Shen, H., *et al.* (2024) Remote Sensing Time Series Analysis: A Review of Data and Applications. *Journal of Remote Sensing*, **4**, Article No. 0285. <https://doi.org/10.34133/remotesensing.0285>
- [33] Sica, F., Pulella, A., Nannini, M., Pinheiro, M. and Rizzoli, P. (2019) Repeat-Pass SAR Interferometry for Land Cover Classification: A Methodology Using Sentinel-1 Short-Time-Series. *Remote Sensing of Environment*, **232**, Article ID: 111277.
<https://doi.org/10.1016/j.rse.2019.111277>
- [34] Braun, A. and Offermann, E. (2022) Polarimetric Information Content of Sentinel-1 for Land Cover Mapping: An Experimental Case Study Using Quad-Pol Data Synthesized from Complementary Repeat-Pass Acquisitions. *Frontiers in Remote Sensing*, **3**, Article 905713. <https://doi.org/10.3389/frsen.2022.905713>
- [35] Bendavid, A. (2008) Comparison of Classification Accuracy Using Cohen's Weighted Kappa. *Expert Systems with Applications*, **34**, 825-832.
<https://doi.org/10.1016/j.eswa.2006.10.022>
- [36] Mandal, D., Kumar, V., Ratha, D., Dey, S., Bhattacharya, A., Lopez-Sanchez, J.M., *et al.* (2020) Dual Polarimetric Radar Vegetation Index for Crop Growth Monitoring Using Sentinel-1 SAR Data. *Remote Sensing of Environment*, **247**, Article ID: 111954.
<https://doi.org/10.1016/j.rse.2020.111954>
- [37] Panchaud, N.H., Enescu, I.I. and Hurni, L. (2017) Smart Cartographic Functionality for Improving Data Visualization in Map Mashups. *Cartographica*, **52**, 194-211.
<https://doi.org/10.3138/cart.52.2.4115>
- [38] Chang, Y.-L., Tan, T.-H., Chen, T.-H., *et al.* (2022) Spatial-Temporal Neural Network

- for Rice Field Classification from SAR Images. *Remote Sensing*, **14**, Article No. 1929. <https://doi.org/10.3390/rs14081929>
- [39] He, Z., Li, S., Wang, Y., Dai, L. and Lin, S. (2018) Monitoring Rice Phenology Based on Backscattering Characteristics of Multi-Temporal RADARSAT-2 Datasets. *Remote Sensing*, **10**, Article No. 340. <https://doi.org/10.3390/rs10020340>
- [40] Singha, C. and Swain, K.C. (2023) Rice Crop Growth Monitoring with Sentinel 1 SAR Data Using Machine Learning Models in Google Earth Engine Cloud. *Remote Sensing Applications. Society and Environment*, **32**, Article ID: 101029. <https://doi.org/10.1016/j.rsase.2023.101029>
- [41] Eriksson, L., Jaworska, J., Worth, A.P., Cronin, M.T.D., McDowell, R.M. and Gramatica, P. (2003) Methods for Reliability and Uncertainty Assessment and for Applicability Evaluations of Classification- and Regression-Based QSARs. *Environmental Health Perspectives*, **111**, 1361-1375. <https://doi.org/10.1289/ehp.5758>
- [42] Veloso, A., Mermoz, S., Bouvet, A., Le Toan, T., Planells, M., Dejoux, J., *et al.* (2017) Understanding the Temporal Behavior of Crops Using Sentinel-1 and Sentinel-2-Like Data for Agricultural Applications. *Remote Sensing of Environment*, **199**, 415-426. <https://doi.org/10.1016/j.rse.2017.07.015>
- [43] Lu, D., Batistella, M., Moran, E. and Mausel, P. (2004) Application of Spectral Mixture Analysis to Amazonian Land-Use and Land-Cover Classification. *International Journal of Remote Sensing*, **25**, 5345-5358. <https://doi.org/10.1080/01431160412331269733>
- [44] Hegde, A.A., Umesh, P. and Tahiliani, M.P. (2024) Comparison of Neural Networks for Binary Spatial Classification of Rice Field by Studying Temporal Pattern Using Dual Polarimetric SAR Measurements. *Journal of the Indian Society of Remote Sensing*, **52**, 2867-2885. <https://doi.org/10.1007/s12524-024-02025-7>
- [45] Haldar, D., Panda, A., Kumar, S. and Chauhan, P. (2023) Monitoring Important Phenological Stages of Rice with Multi-Season Rice Crop Profile Using Indian SCATSAT-1 Data. *Med Discoveries*, **2**, Article No. 1034. <https://doi.org/10.52768/2993-1142/1034>